The V5 Domain of Protein Kinase C Plays a Critical Role in Determining the Isoform-Specific Localization, Translocation, and Biological Function of Protein Kinase C-δ and -ε

Qiming Jane Wang,[1] Ganwei Lu,[5] Walter A. Schlapkohl,[2] Axel Goerke,[3] Christer Larsson,[4] Harald Mischak,[3] Peter M. Blumberg,[1] and J. Frederic Mushinski[2]

[1]Laboratory of Cellular Carcinogenesis and Tumor Promotion and [2]Laboratory of Genetics, National Cancer Institute, Bethesda, MD; [3]Abteilung Nephrologie, Hannover Medical School, Hannover, Germany; and [4]Department of Laboratory Medicine, Division of Molecular Medicine, Lund University, Malmo, Sweden; and [5]Department of Pharmacology, University of Pittsburgh, Pittsburgh, PA

Abstract

The catalytic domain of overexpressed protein kinase C (PKC)-δ mediates phorbol 12-myristate 13-acetate (PMA)-induced differentiation or apoptosis in appropriate model cell lines. To define the portions of the catalytic domain that are critical for these isozyme-specific functions, we constructed reciprocal chimeras, PKC-δ/εV5 and -ε/δV5, by swapping the V5 domains of PKC-δ and -ε. PKC-δ/εV5 failed to mediate PMA-induced differentiation of 32D cells, showing the essential nature of the V5 domain for PKC-δ's functionality. The other chimera, PKC-ε/δV5, endowed inactive PKC-ε with nearly all PKC-δ's apoptotic ability, confirming the importance of PKC-δ in this function. Green fluorescent protein (GFP)-tagged PKC-δV5 and -ε/δV5 in A7r5 cells showed substantial basal nuclear localization, while GFP-tagged PKC-ε and -δ/εV5 showed significantly less, indicating that the V5 region of PKC-δ contains determinants critical to its nuclear distribution. PKC-ε/δV5-GFP showed much slower kinetics of translocation to membranes in response to PMA than parental PKC-ε, implicating the PKC-εV5 domain in membrane targeting. Thus, the V5 domain is critical in several of the isozyme-specific functions of PKC-δ and -ε.

Introduction

Protein kinase C (PKC) is a family of at least 10 serine/threonine kinases. As major mediators of signal transduction pathways, PKCs have been shown to regulate a diverse set of biological functions, such as cell growth, differentiation, apoptosis, transformation, and tumorgenicity (1–5). All PKCs are composed of two functionally distinct halves, a NH_2-terminal regulatory domain and a COOH-terminal catalytic domain. Conserved (C1–C4) and variable (V1–V5) regions alternate throughout the primary sequence (Fig. 1). To keep the kinases in an inactive state, the regulatory domain of PKC binds to and inhibits the catalytic domain through a pseudosubstrate region (6). PKC isozyme specificity is determined, in large part, by its subcellular localization (7–9). On activation by the binding of diacylglycerol or phorbol 12-myristate 13-acetate (PMA) to the regulatory domain, the pseudosubstrate region is withdrawn from the kinase domain, leaving the kinase active to phosphorylate its preferred substrate (1, 10).

Two structurally similar isozymes of the same "novel" class of PKCs, PKC-δ and -ε, mediate quite contrasting physiological effects. Overexpressed PKC-ε stimulates growth and is oncogenic in mouse, rat, and human fibroblasts as well as in rat colon epithelial cells (3–5). In contrast, PKC-δ inhibits cell growth in fibroblasts (3, 11) and induces differentiation in promyelocytic cells (2). PKC-δ, when overexpressed in vascular smooth muscle cells, induces apoptosis in response to PMA treatment, while PKC-ε does not (12). In salivary gland acinar cells, PKC-δ is essential for etoposide-induced apoptosis (13).

To understand the structural basis for these isozyme-specific effects, mutants and chimeras have been constructed to explore the functional significance of the various PKC domains. Using PKC-δ/ε and -ε/δ chimeras in which regulatory and catalytic domains from PKC-δ and -ε had been exchanged, we showed that the catalytic domain of PKC-δ determined the macrophage differentiation of mouse promyelocytes induced by PMA (14) and that the catalytic domain of PKC-ε was responsible for its tumorgenicity in NIH 3T3 cells (15). In addition, the catalytic domain of PKC-δ was found to mediate etoposide-induced apoptosis (16) and the protection by bryostatin 1 of PKC-δ from down-regulation (17). In other studies, the regulatory domain of PKC-ε was associated with enhanced growth rate, while the regulatory domains of PKC-δ and -α were associated with the inhibition of proliferation (18). These studies, however, are not mutually exclusive; in fact, the roles of the variable domains in each isoform are likely to be context specific.

In the present study, we sought to define further the structural elements that determine the specificity of the catalytic domain by focusing on the COOH-terminal 65 (PKC-δ) and 68 (PKC-ε)

Received 6/16/03; revised 11/26/03; accepted 12/17/03.
Note: Present address of Q. J. Wang: Department of Pharmacology, University of Pittsburgh, Pittsburgh, PA.
The costs of publication of this article were defrayed in part by the payment of page charges. This article must therefore be hereby marked advertisement in accordance with 18 U.S.C. Section 1734 solely to indicate this fact.
Requests for reprints: J. Frederic Mushinski, NIH, Building 37, Room 3134C, 37 Convent Drive, MSC-4256, Bethesda, MD 20892-4256. Phone: (301) 496-5260; Fax: (301) 402-1031. E-mail: jm8p@nih.gov

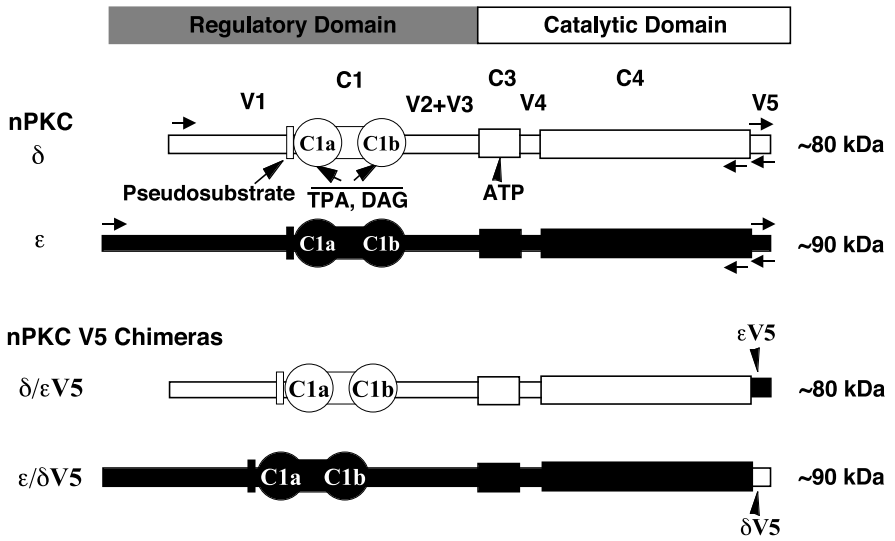

FIGURE 1. Structure of PKC-δ and -ε and PKC-δ/εV5 and -ε/δV5 chimeras. Schema of wild-type and chimeric PKCs and their domains. *Short horizontal arrows,* PCR primers used in making the chimeric constructs.

amino acids, the V5 regions of PKC-δ and -ε, respectively. Interest in the V5 region is driven by the fact that PKC-βI and -βII, which differ only in the V5 region, translocate to distinct subcellular locations when activated in the same cell type (9, 19) and are associated with different physiological functions (20–23). In PKC-δ and -ε, the V5 domains show higher sequence differences compared with other variable regions of the catalytic domain. In the present study, we overexpressed a pair of reciprocal chimeric PKC cDNAs composed of >90% wild-type PKC-δ or -ε but with the V5 domains (the COOH terminus ~10% of each isoform) exchanged. The contribution of the V5 domain to intracellular targeting and to isotype-specific functions was studied in appropriate model cell systems.

Results

Expression and Translocation of PKCs and Chimeras Fused to Green Fluorescent Protein in NIH 3T3 Cells

Because our earlier immunohistochemical studies of PKC-δ and -ε showed different subcellular distribution and patterns of translocation in response to PMA activation for NIH 3T3 overexpressers (9), we examined the subcellular targeting of PKC-δ/εV5 and -ε/δV5 fused to green fluorescent protein (GFP) and compared it with that of GFP-tagged wild-type PKC-δ and -ε by live cell imaging.

PKC-δ/εV5 and -ε/δV5 were generated by PCR as illustrated in Fig. 1 and were subcloned into a pEGFP-N1 vector to produce COOH-terminal GFP fusion proteins. The GFP fusion constructs were then transiently expressed in NIH 3T3 cells. The immunoreactivity of the transfected cells was examined by Western blotting. As illustrated in Fig. 2A, all GFP fusion proteins were identified by a monoclonal anti-GFP antibody as specific bands with the expected molecular sizes, 105 kDa for PKC-δ-GFP and -δ/εV5-GFP and 115 kDa for PKC-ε-GFP and -ε/δV5-GFP. A polyclonal anti-PKC-δ COOH-terminal antibody likewise recognized the PKC-δ-GFP and -ε/δV5-GFP but did not recognize PKC-ε-GFP and -δ/εV5-GFP (data not shown). GFP alone expressed in NIH 3T3 cells showed uniform distribution within nucleoplasm and cytoplasm and no translocation after treatment with 1 μM PMA (data not shown). In addition, no apparent degradation was seen for either wild-type or chimeric PKCs during a 40-min treatment with PMA or bryostatin 1 (data not shown). Therefore, the pattern of translocation truly reflected the behavior of the intact fusion protein.

In the absence of activators, both PKC-δ-GFP and -ε-GFP were present in the cytosol but only PKC-δ-GFP was also visible in the nucleus (Fig. 2B). PKC-δ/εV5-GFP and -ε/δV5-GFP, similar to PKC-ε-GFP, were only observed in the cytosol. A quantitative determination of nuclear PKC content showed that PKC-ε could be detected in the nucleus. However, as illustrated in Fig. 2C, the ratio of nuclear/cytoplasmic distribution of PKC-δ-GFP was approximately twice that of PKC-ε-GFP and -δ/εV5-GFP, indicating that the V5 domain of PKC-δ plays an important role in determining the nuclear distribution of PKC-δ. It was not sufficient, however, in NIH 3T3 cells to induce the PKC-ε/δV5-GFP chimera to enter the nucleus to the extent seen for PKC-δ.

To characterize the role of V5 region in membrane targeting of PKC-δ and -ε, we imaged the PMA-induced plasma membrane translocation of the GFP-tagged wild-type PKCs and chimeras in live cells then performed quantitative determination of changes of the green fluorescent signal at the plasma membrane. As shown in Fig. 2, B and D, PKC-δ-GFP behaved as reported previously in response to 1 μM PMA for 20 min (*i.e.*, by rapidly translocating to the plasma and nuclear membranes; 24). PKC-ε-GFP responded to PMA treatment by translocating to the plasma membrane only, reaching the maximum ~15 min after treatment. The PKC-δ/εV5-GFP chimera exhibited the slow kinetics of translocation to the plasma membrane as seen for PKC-ε, although not as extensive, and little translocation to the nuclear membrane. PKC-ε/δV5-GFP showed the slowest

plasma membrane translocation kinetics of all, requiring 15–20 min to achieve maximal plasma membrane translocation. Thus, the V5 domain is critical to the isoform-specific features of PMA-induced membrane translocation of both PKC-δ and -ε.

Expression of Wild-Type and Chimeric PKC in 32D Cells

PCR-generated PKC-δ/εV5 and -ε/δV5 were first subcloned into the pLTR vector for expression of untagged proteins and then into the pcDNA vector for the expression of Myc epitope-tagged or untagged proteins in mammalian systems. After transfection of the constructs into 32D cells and subsequent selection, pools of 32D cells that stably expressed PKC-δ/εV5 and -ε/δV5 were obtained. We found that different expression vectors often yielded different steady-state levels of wild-type and chimeric PKCs in 32D cells. Because levels of protein expression may affect protein function in cells, we sought lines of 32D cells that expressed as similar as possible levels of wild-type and chimeric PKCs, irrespective of the vector. We made certain, however, that when these empty vectors were expressed in 32D cells, none influenced the behavior of 32D cells with or without PMA treatment (data not shown). Thus, we obtained L-δ/εV5, the 32D line that expressed PKC-ε/δV5 in pLTR vector, and D-δ/εV5-*myc*, -ε/δV5-*myc*, and -ε/δV5, the 32D lines that expressed the V5 chimeras with or without Myc tag in pcDNA vectors. Due to technical difficulties, we did not obtain the corresponding untagged L-ε/δV5 and D-ε/δV5 lines.

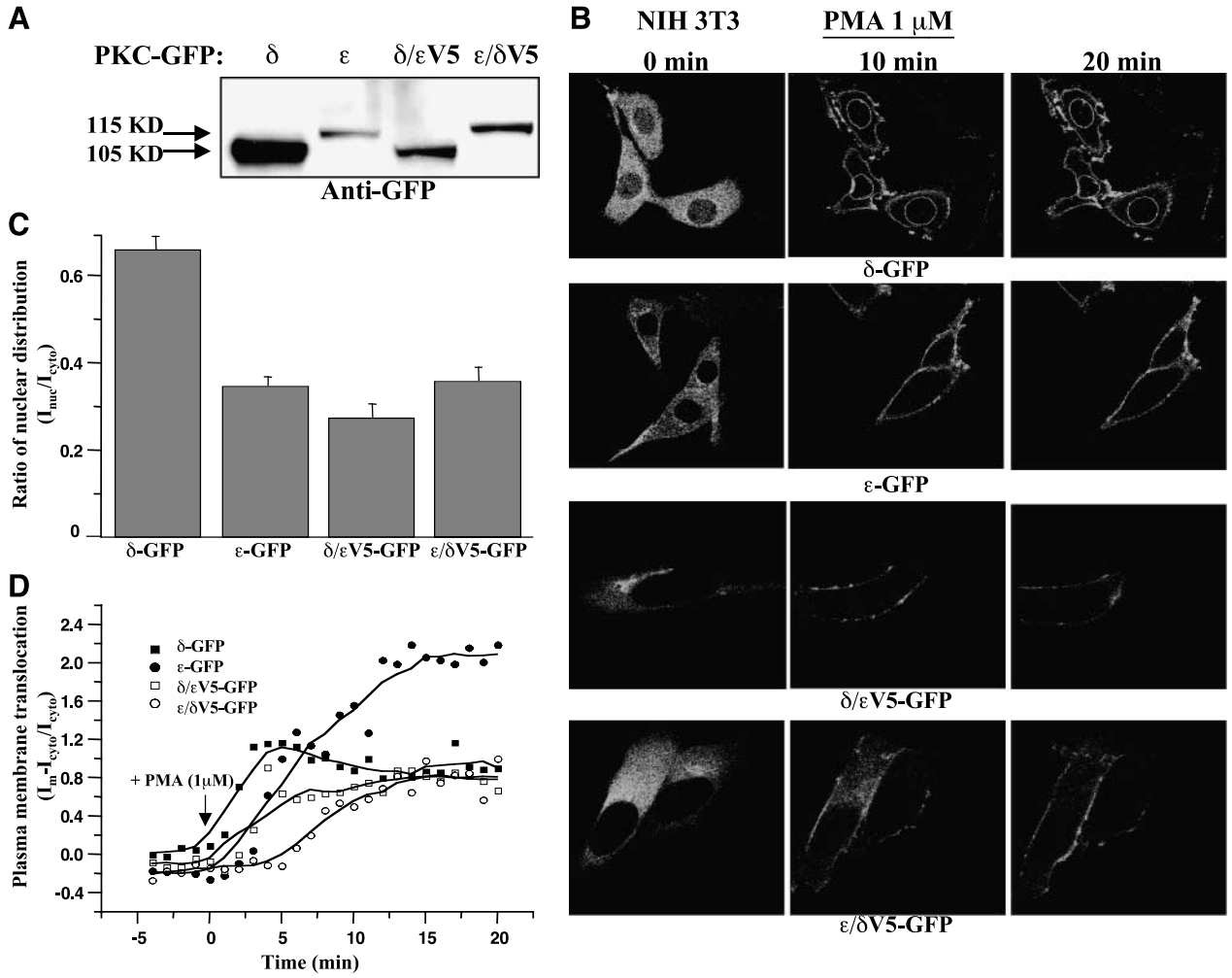

FIGURE 2. Translocation of GFP-tagged wild-type and V5 chimeric PKCs in response to PMA in NIH 3T3 cells. **A.** Western blot analysis of PKC-δ-GFP, -ε-GFP, -δ/εV5-GFP, and -ε/δV5-GFP transiently expressed in NIH 3T3 cells. Fusion proteins were detected with an anti-GFP antibody. **B.** Translocation of PKC-δ-GFP, -ε-GFP, -δ/εV5-GFP, and -ε/δV5-GFP in NIH 3T3 cells in response to PMA (1 μM). Cells were imaged every minute for a total of 20 min in the presence of PMA, with images at 0, 10, and 20 min after PMA treatment. Representative of all fields in each of three similar experiments. **C.** Quantitative determination of the distribution of GFP-tagged parental and chimeric PKC proteins in the nucleus of untreated NIH 3T3 cells that overexpressed various PKC constructs. Ratio of nuclear/cytoplasmic distribution was calculated as the ratio of I_{nucl}/I_{cyto}, where I_{nucl} is the mean fluorescent intensity in the nucleus in a given area and I_{cyto} is the mean fluorescent intensity in a comparable area of the cytoplasm. *Columns,* average of three experiments with 5–10 cells evaluated in each experiment. **D.** Kinetic analysis of GFP-tagged PKC proteins at the plasma membrane of NIH 3T3 cells in response to PMA treatment. Ratio of plasma membrane translocation was calculated as the ratio of $(I_m - I_{cyto})/I_{cyto}$, where I_m is the mean fluorescent intensity on the plasma membrane in a given area and I_{cyto} is the mean fluorescent intensity in a comparable area of the cytoplasm. *Points,* average of three experiments with one to two cells evaluated in each experiment.

As illustrated in Fig. 3, the PKC-δ/εV5 chimeric protein in 32D cells, identified by an anti-PKC-ε COOH-terminal antibody, had the same electrophoretic mobility as the endogenous PKC-δ (Fig. 3A), while the PKC-ε/δV5 chimeric protein, identified by the anti-PKC-δ COOH-terminal antibody, was the same size as the endogenous PKC-ε (Fig. 3B). Myc-tagged PKC-δ/εV5 and -ε/δV5 in pcDNA-based clones were detected by an anti-Myc antibody (Fig. 3C) and distinguished these exogenous PKCs from endogenous PKCs.

Because levels of overexpression relative to the endogenous expression may be a contributing factor to PKC-δ-mediated 32D differentiation, we compared the levels of overexpressed PKC-δ/εV5 and -ε/δV5 relative to the endogenous PKC-δ and the overexpressed PKC-δ using an anti-NH_2-terminal PKC-δ antibody (Fig. 3D). M-δ, a previously established 32D line with reduced PKC-δ overexpression, is as potent as L-δ in differentiation (Fig. 4) and is included for comparison. As illustrated in Fig. 3D, the levels of PKC-δ/εV5 were comparable to the levels of PKC-δ in M-δ and were substantially higher than the endogenous PKC-δ, indicating that the lack of functionality of L-δ/εV5 and D-δ/εV5-*myc* was not due to low levels of expression relative to endogenous PKC-δ. We also found comparable levels of PKC-ε/δV5 relative to the endogenous PKC-ε in the control pcDNA line or the overexpressed PKC-ε in L-ε using an anti-NH_2-terminal PKC-ε antibody (Fig. 3D). Protein loading was controlled by developing the same blots with an anti-actin antibody.

Overexpression of PKC-δ/εV5 and -ε/δV5 Did Not Induce Differentiation of 32D Cells in the Presence of PMA

The 32D cells that overexpress PKC-δ, but not those that overexpress PKC-ε, differentiate into macrophages in the presence of PMA (2), and this property was shown to reside in the catalytic domain of PKC-δ (14). Thus, 32D lines overexpressing wild-type and chimeric PKC-δ and -ε, L-δ, -ε, and -δ/εV5, and D-ε/δV5-*myc* were treated with 10 ng/ml PMA for 10 h, and their differentiation into macrophages was evaluated by morphology and by the expression of the Mac-1 and Mac-3 surface markers that are characteristic of macrophages. Only PMA-treated L-δ acquired the phenotypic features of macrophages: large cells with poorly defined plasma membrane and numerous cytoplasmic vacuoles (Fig. 5). PMA-treated L-εV5 and -δ/εV5 and D-ε/δV5-*myc* retained the typical promyelocyte morphology of 32D cells: small round cells with well-defined plasma membrane (2, 14). These data suggested that the V5 domain of PKC-δ was required to mediate macrophage

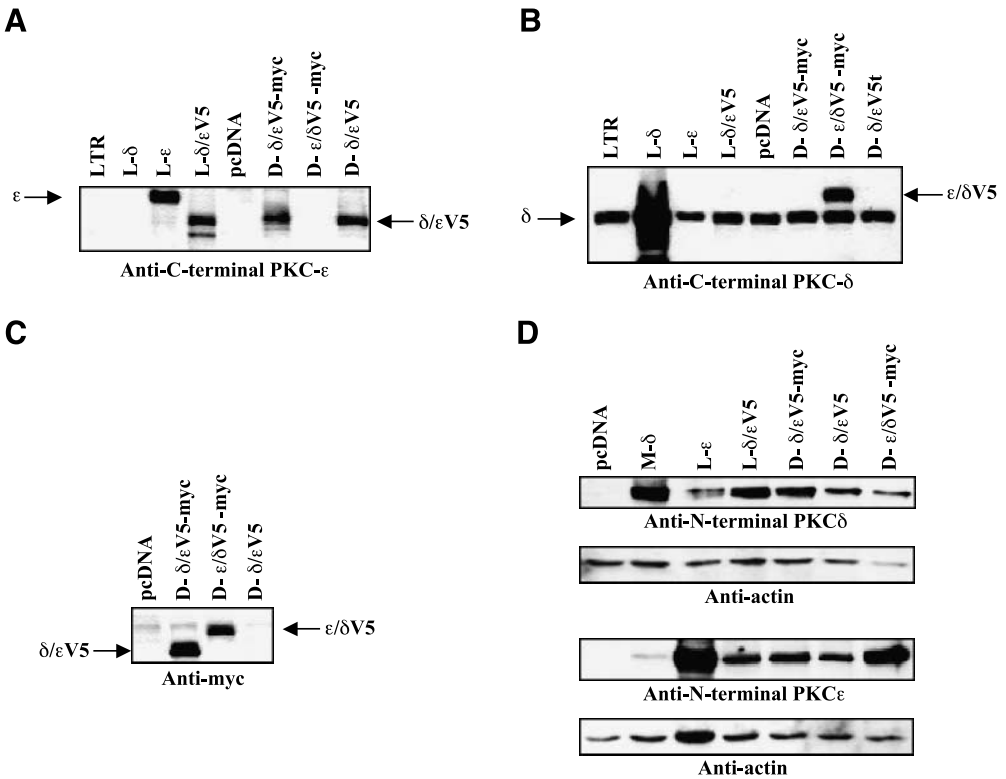

FIGURE 3. Stable expression of PKC-δ, -ε, -δ/εV5, and -ε/δV5 in 32D cells. Western blot analysis of 32D cells that stably expressed the native and chimeric PKCs was described under "Materials and Methods." **A.** Overexpressed PKC-δ/εV5 and -ε were detected with an anti-PKC-ε COOH-terminal antibody. **B.** Endogenous and overexpressed PKC-δ as well as PKC-ε/δV5 were detected with an anti-PKC-δ COOH-terminal antibody. Bands of degraded PKC proteins can be seen in the high-level PKC-δ overexpresser. **C.** 32D cells expressing Myc-tagged PKC-δ/εV5 and -ε/δV5 chimeras were detected with an anti-Myc antibody. **D.** Overexpressed PKC-δ/εV5 *versus* endogenous and overexpressed PKC-δ was detected with an anti-PKC-δ NH_2-terminal antibody. Overexpressed PKC-ε/δV5 *versus* endogenous and overexpressed PKC-ε was detected with an anti-PKC-ε NH_2-terminal antibody. Estimates of protein loading were obtained by blotting with anti-actin antibody in each case. Representative of three independent experiments.

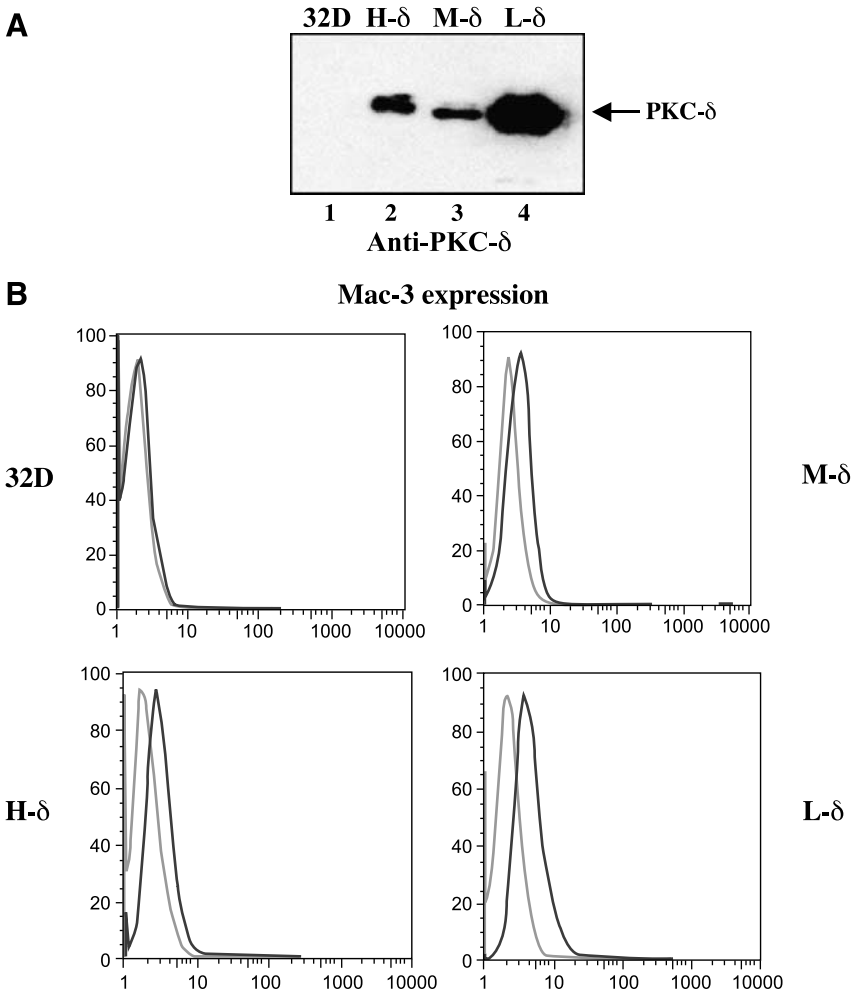

FIGURE 4. Mac-3 stains positive on PKC-δ-overexpressing 32D cells treated with PMA regardless of PKC-δ expression level. **A.** Western blot of 32D cell lysates obtained before PMA treatment and developed with anti-PKC-δ. *Lane 1,* untransfected 32D cell lysate. *Lanes 2*, *3*, and *4,* 32D cells showing varying amounts of PKC-δ protein. *Lane 2,* PKC-δ with slightly higher molecular weight because this protein is fused to a NH_2-terminal hemagglutinin epitope tag. **B.** Flow cytometric analysis of the same cells before (*gray*) and after (*black*) 6-h treatment with 50 nM PMA.

differentiation because PKC-δ with an exchanged V5 region, PKC-δ/εV5, completely lost its ability to induce macrophage differentiation. However, the δV5 domain was not sufficient to make a PKC isoform induce differentiation because PMA treatment of cells expressing PKC-ε/δV5 did not lead to morphological evidence of macrophage differentiation (Fig. 5) or increased expression of the Mac-1 and Mac-3 macrophage markers (Fig. 6). Only L-δ showed a significant increase in Mac-1 and Mac-3, indicating maturation toward macrophages (Fig. 6). There were no apparent changes in the expression of macrophage surface markers in lines that overexpress PKC-ε and V5 chimeras after 20 h of PMA treatment at 10 ng/ml (Fig. 6) and 50 ng/ml (data not shown), indicating that the V5 domain of PKC-δ was indispensable for PKC-δ to mediate PMA-induced macrophage differentiation.

The 32D cells differentiate into macrophages only in the presence of overexpressed PKC-δ (2), implying that endogenous levels of PKC-δ are not high enough to induce differentiation. Thus, levels of PKC-δ overexpression relative to the endogenous expression may affect differentiation. To address this issue, we overexpressed PKC-δ in 32D cells under the control of the metallothionein promoter and cytomegalovirus promoter, generating two stable lines, M-δ and H-δ. Both M-δ and H-δ showed lower PKC-δ expression than L-δ, and both exhibited macrophage features that are comparable with those of L-δ (Fig. 4). This demonstrates that very high levels of overexpression are not required for differentiation. In addition, as shown in Fig. 3D, the results obtained with antibodies to the NH_2 termini of PKC-δ and -ε showed that the levels of V5 chimeras in L-δ/εV5 and D-ε/δV5-*myc* were comparable with the levels of overexpressed PKC-δ that were capable of inducing differentiation. Therefore, we excluded the formal possibility that differentiation had failed because neither chimera achieved the very high levels of exogenous PKC expression achieved only in L-δ.

To exclude the possibility that the COOH-terminal Myc epitope may interfere with the function of the V5 chimeras, we constructed pcDNA-δ/εV5, in which a stop codon was inserted before the Myc epitope. When expressed in 32D cells, designated

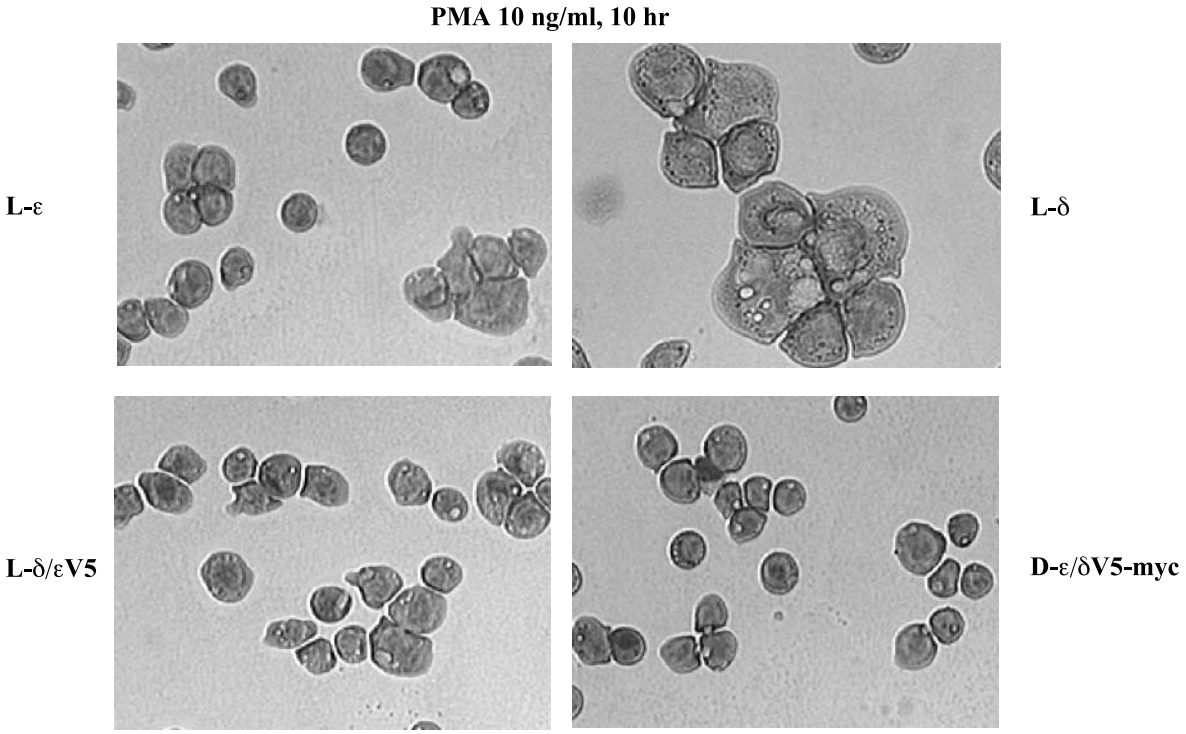

FIGURE 5. Morphology of wild-type and chimeric PKC overexpressers after PMA treatment. 32D lines that express PKC-δ (*L-δ*), PKC-ε (*L-ε*), and chimeras (*L-δ/εV5* and *D-ε/δV5-myc*) treated with 10 ng/ml PMA for 10 h. The cells were applied to uncoated glass microscope slides using cytocentrifugation and then stained with Giemsa. Photographs of representative fields were taken using an inverted light microscope under ×630 magnification. Data from one of three similar experiments.

as D-δ/εV5, at levels similar to those in D-δ/εV5-*myc* and L-δ/εV5 (Fig. 3B), no difference in behavior was observed among these cell lines (data not shown), implying that the COOH-terminal Myc tag had no effect on the function of the chimeric proteins expressed in 32D cells. Therefore, their function reflects the nature of the intact wild-type or chimeric proteins.

Overexpression of PKC-ε/δV5 Was More Apoptotic Than PKC-δ/εV5 in A7r5 Cells on PMA treatment

Overexpression of PKC-δ but not PKC-ε in A7r5 rat smooth muscle cells induces apoptosis on PMA treatment, an effect that appears to require membrane translocation (12). To test whether the V5 domain contributes to the apoptotic effect of PKC-δ, we overexpressed GFP-tagged PKC-δ, -ε, -δ/εV5, and -ε/δV5 in A7r5 cells. Cells were then treated with 2 μm PMA for 4 h. The apoptotic response was first determined by staining nuclei with Hoechst 33342 and examining them for the appearance of chromatin condensation and nuclear disintegration, as used in our earlier publication (12). Cells overexpressing PKC-δ-GFP showed the highest percentage of apoptotic cells in response to PMA treatment, while cells overexpressing PKC-ε-GFP, like GFP alone, showed few apoptotic nuclei (Fig. 7A). Strikingly, A7r5 cells overexpressing PKC-ε/δV5-GFP showed a high percentage of apoptotic cells, one that was not statistically different from that of the parental PKC-δ. In contrast, overexpression of PKC-δ/εV5-GFP was two-thirds less effective in inducing apoptosis, a significant ($P < 0.05$) difference.

These data were confirmed by the terminal deoxynucleotidyl transferase-mediated nick end labeling (TUNEL) assay of apoptosis, as shown in Fig. 7B. In this assay, the chimeric PKC-ε/δV5-GFP did not quite achieve the levels of apoptosis produced by PKC-δ-GFP, but the addition of merely the COOH-terminal 10% of PKC-δ to the completely inactive PKC-ε rendered the chimera nearly as apoptogenic as PKC-δ-GFP. In addition, Annexin V assay (data not shown) of transiently transfected cells also showed comparable data, confirming that all the cells that exhibited GFP fluorescence and nuclear abnormalities showed Annexin V evidence of apoptosis. The above data clearly indicate that the V5 domain of PKC-δ contributes significantly to PKC-δ-induced apoptosis in vascular smooth muscle cells in response to PMA treatment.

It has been demonstrated that the V5 region of PKC-δ contains a nuclear localization signal and that nuclear PKC-δ plays an important role in apoptosis (16, 25). Thus, it is plausible that the V5 region of PKC-δ contributes to apoptosis by targeting PKC-δ and -ε/δV5 chimera to the nucleus of A7r5 cells. To investigate this possibility, GFP-tagged PKC-δ and -ε and PKC-δ/εV5 and -ε/δV5 chimeras were transiently transfected into A7r5 cells. The ratio of nuclear/cytoplasmic distribution of GFP-tagged PKCs was quantified at basal state. As illustrated in Fig. 8, PKC-δ-GFP showed a greater nuclear distribution than PKC-ε-GFP ($P < 0.05$). Interestingly, by switching to the V5 domain of PKC-δ, PKC-ε/δV5 exhibited the highest ratio of nuclear localization of all in A7r5 cells ($P < 0.05$). In contrast,

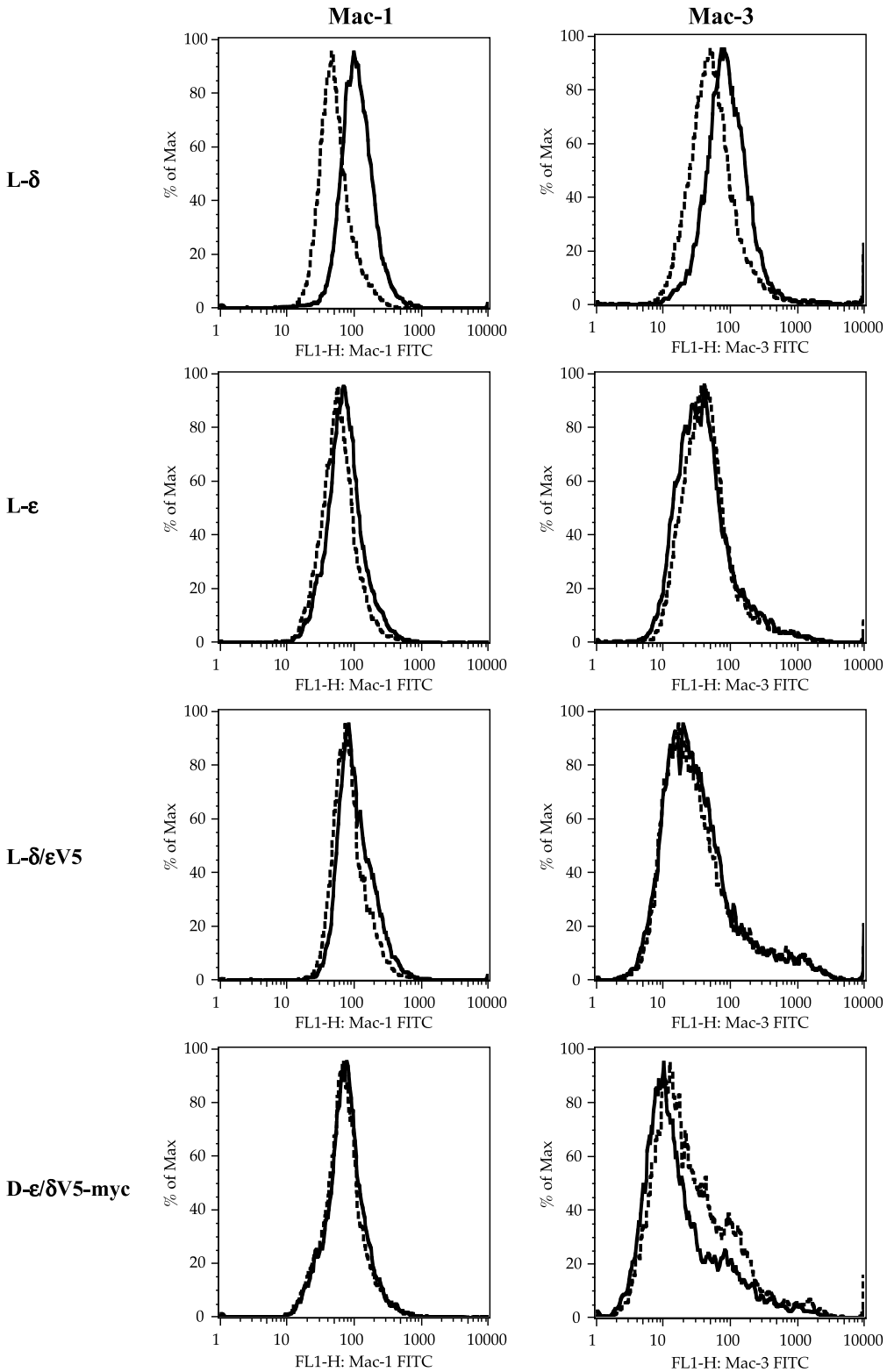

FIGURE 6. Flow cytometry analysis of the macrophage differentiation makers (Mac-1 and Mac-3) on wild-type and chimera overexpressers. Cells were treated with or without 10 ng/ml PMA for 10 h and stained with FITC-labeled antibodies against Mac-1 and Mac-3. *Dashed lines,* peaks for the specific Mac-1 or Mac-3 fluorescence with no PMA treatment; *solid lines,* peaks for the fluorescence intensity after PMA treatment. The experiment was repeated four times. Data from a representative experiment.

loss of the V5 region of PKC-δ in PKC-δ/εV5 caused a significant ($P < 0.05$) reduction in nuclear localization. Thus, the nuclear distribution of PKC-δ and -ε and their V5 chimeras correlated well with their apoptotic activity, suggesting that the isoform-selective effects of PKC-δ and -ε are, at least in part, due to the differential nuclear localization conferred by the V5 region.

Discussion

Studies using PKC regulatory/catalytic domain chimeras have underscored the complexity of PKC functions in relation to its structural domains. In previous reports, we and others showed that certain features of isozyme-specific PKC functions could be attributed to the catalytic domain only. These include the PKC-δ-mediated PMA-induced macrophage differentiation of 32D cells (14), the tumorigenicity of PKC-ε-overexpressing NIH 3T3 cells (15), the PKC-βII-mediated growth promotion in K-562 cells (26), and the protection of PKC-δ from down-regulation induced by bryostatin 1 in NIH 3T3 cells (17). However, in some cases, both the regulatory and the catalytic domains contribute to the isoform-specific effects (15, 18, 27). Further mapping of the structural domains beyond the catalytic and regulatory regions is essential to clearly determine the function of each structural domain and to understand how individual domains interact with each other to regulate PKC function.

Previous studies on the role of the V5 domain of PKC in isoform-selective functions had focused mainly on the PKC-βI and -βII isoforms. The two PKC isoforms are differentially spliced variants of the same gene and therefore differ only in their COOH-terminal V5 region. In a previous study (9), we showed that PKC-βI and -βII translocated to different intracellular compartments following PMA treatment. Others also showed that PKC-βI and -βII are localized differentially both in their active and inactive states (28, 29). The isolated V5

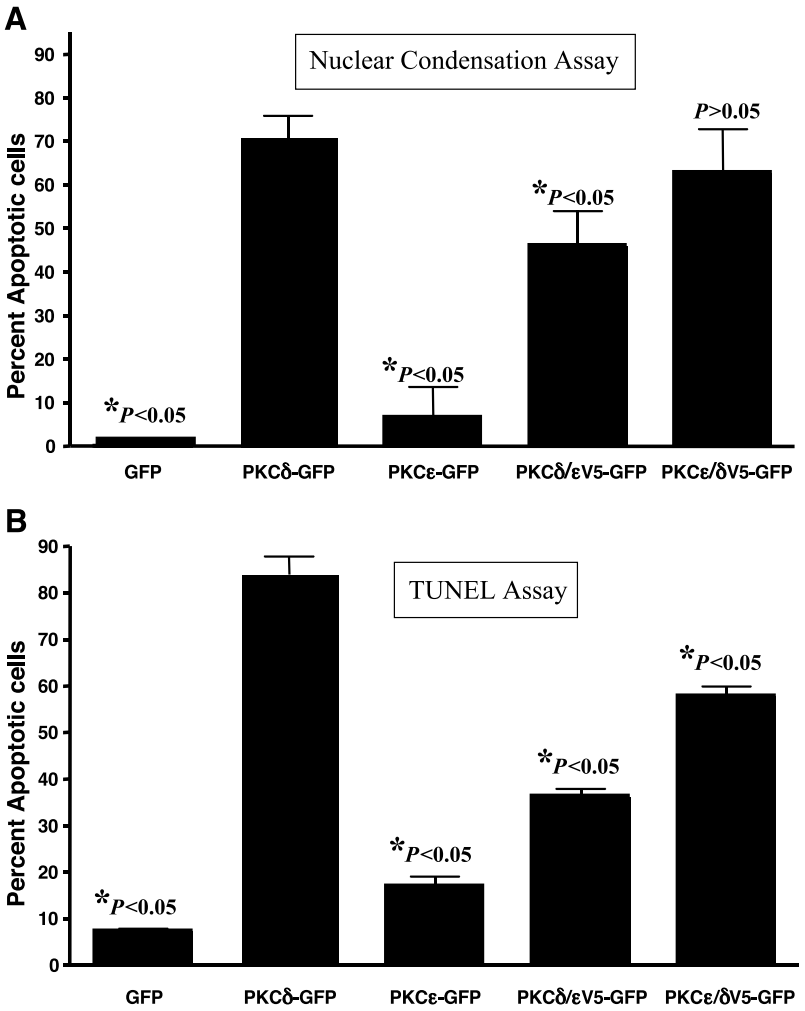

FIGURE 7. Apoptotic response to PMA in A7r5 cells transiently overexpressing GFP fusions of wild-type PKC and the V5 chimeras. Two quantitative analyses of the apoptotic response were performed on each transfectant after treatment with 2 μM PMA for 4 h. *Columns,* mean of two to five experiments; *bars,* SEM. At least 100 cells were counted in each experiment. Results are percentages of apoptotic cells out of all GFP-positive cells. *, $P < 0.05$ (one-way ANOVA), significant differences between the apoptotic responses induced in PKC-δ-GFP overexpressers compared with all other overexpressers. **A.** Apoptotic cells were defined as cells bearing condensed or fragmented nuclei after staining with Hoechst 33342. **B.** Apoptotic cells were detected with the TUNEL assay.

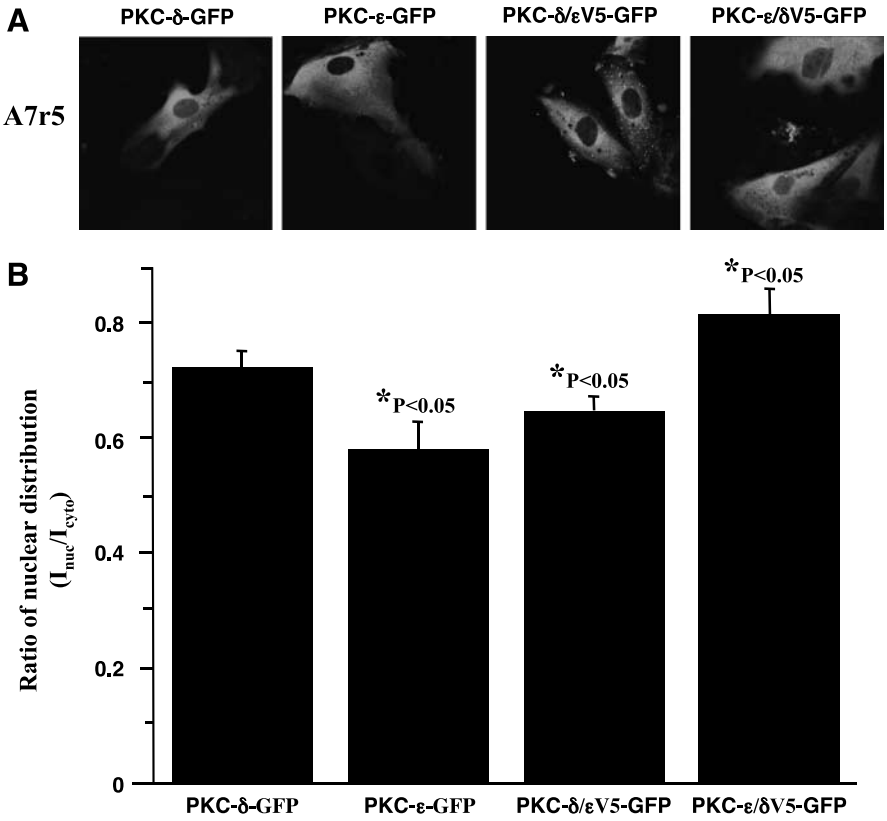

FIGURE 8. Nuclear distribution of GFP-tagged wild-type and V5 chimeric PKCs in basal state of A7r5 cells. **A.** Intracellular distribution of PKC-δ-GFP, -ε-GFP, -δ/εV5-GFP, and -ε/δV5-GFP in A7r5 cells. Representative of all fields in each of three similar experiments. **B.** Quantitative measurements of the nuclear distribution of GFP-tagged parental and chimeric PKCs. Ratio of nuclear/cytoplasmic distribution was calculated as the ratio of I_{nucl}/I_{cyto}, where I_{nucl} is the mean fluorescent intensity in the nucleus in a given area and I_{cyto} is the mean fluorescent intensity in a comparable area of the cytoplasm. *Columns,* average of three experiments with 30–50 cells evaluated in total.

domain of PKC-βI suppressed proliferation of neuroblastoma cells more than that from PKC-βII (23). Chimeras generated between various regions of PKC-α and -βII demonstrated that the COOH-terminal 13 amino acids from PKC-βII was sufficient to confer the nuclear translocation and lamin B phosphorylation characteristic of PKC-βII (22, 26). Further studies by these authors showed a selective interaction between this region and the nuclear membrane lipid, phosphatidylglycerol, which may account for the specific nuclear function of PKC-βII (22). In addition, Stebbins and Mochly-Rosen (30) showed that the same V5 region in PKC-βII bound to the selective βII-anchoring protein, RACK1, and the inhibition of this interaction by peptides derived from the βIIV5 region abolished PKC-βII-mediated cardiac myocyte hypertrophy. Meanwhile, a V5 domain deletion mutant of PKC-βII inhibited insulin-stimulated 2-deoxyglucose uptake in L6 rat skeletal muscle cells (31). These studies pointed to a critical role of V5 domain of PKC-βII in its isoform-specific functions. In this study, we investigated whether the V5 region of PKC-δ would confer PKC-δ-specific characteristics on PKC-ε or compromise the characteristics of wild-type PKC-ε. A similar rationale applied for the V5 region of PKC-ε.

Given that the V5 domain of PKC-βII contributed to its isoform-specific functions through the control of its intracellular distribution, we examined the intracellular localization of PKC-δ, -ε, -δ/εV5, and -ε/δV5 in appropriate model cell lines, focusing primarily on their nuclear distribution. More nuclear PKC-ε/δV5 than nuclear PKC-δ/εV5 in A7r5 cells indicated that the V5 domain of PKC-δ contributed to its nuclear distribution. The nuclear PKC-δ is tightly coupled to a series of PKC-δ-specific functions in cells, especially that of apoptosis (32). PKC-δ was found to accumulate in the nuclei of C5 rat parotid cells and C6 glioma cells in response to inducers of apoptosis such as etoposide (16, 33), and the importation of PKC-δ to the nucleus is required for apoptosis in C5 rat parotid cells (16). Nuclear targets of PKC-δ have been identified such as the DNA-dependent protein kinase (34) and the lamin proteins (35), both of which are important apoptotic mediators. In the data reported here, we found that the δV5 region contained sufficient structure to mediate PMA-induced apoptosis of A7r5 smooth muscle cells (Fig. 7) and contributed to increased nuclear localization (Fig. 8). These results are consistent with those of DeVries *et al*. (16) who demonstrated the presence of a functional nuclear localization signal in the COOH-terminal region of rat PKC-δ. This motif is identical in the mouse PKC-δV5 (36) used in our study. Interestingly, mouse PKC-ε has a similar sequence in the same area of its V5 domain, but less nuclear PKC-ε-GFP was seen in these cells (Figs. 2 and 8), and PKC-ε is not thought to be involved in etoposide-induced apoptosis of salivary gland acinar cells (13). Nonetheless, the PKC-εV5 did contribute to

the physiology of PKC-ε, inasmuch as PKC-ε/δV5 showed much slower kinetics of PMA-induced translocation to membranes than PKC-ε. Although the mechanism involved is not yet known, we conclude that the εV5 domain plays a role, either direct or indirect, in the membrane targeting induced by PMA.

We evaluated the functional roles of V5 domain of PKC-δ and -ε in two cell types. We first studied 32D cells, a line that differentiates into macrophages in response to PMA when PKC-δ, but not PKC-ε, is overexpressed. Cells overexpressing PKC-δ/εV5 and -ε/δV5 were unable to differentiate into macrophages in response to PMA treatment at different doses. In addition, both 32D-δ/εV5 and -ε/δV5 cells proved to be fast growing and low in adherence in the presence of PMA, characteristics of undifferentiated promyelocytes and closely resembling the PKC-ε overexpresser and parental 32D cells. These results indicate that the V5 domain of PKC-δ is necessary for the PMA-induced differentiation of 32D cells, although in the context of the PKC-ε/δV5 chimera, the V5 domain was unable to induce differentiation. In agreement with these findings, the apoptotic effect of PKC-δ in the A7r5 rat aortic smooth muscle cell line can be attributed to its V5 domain. It also seems to be dependent, in large measure, on the ability of the effector molecule to translocate to the membrane location of its protein target (12). The fact that PKC-ε/δV5 was able to induce an apoptotic response similar in magnitude to PKC-δ suggests that V5 domain contains most of the critical determinants for this effect.

At present, the molecular basis underlying the lack of differentiation for 32D cells overexpressing PKC-δ/εV5 and -ε/δV5 is unknown. Possibilities that may account for this effect are their differential localization in cells, the lack of critical intramolecular interactions, and any change of their phosphorylation status. Edwards *et al*. (37) showed that phosphorylation at Thr^{641} in PKC-βII was essential for both its catalytic function and its correct subcellular localization, while phosphorylation at Ser^{660} regulated its ability to bind to substrate and to Ca^{2+} (38). It is unknown how these phosphorylation sites in PKC-δ and -ε contribute to their function and localization and whether substitution with foreign V5 domains influences this phosphorylation. This question will be the subject of our next series of experiments. Moreover, mutants at Ser^{660} in PKC-βII implied an interaction between the V5 and the C2 domains that cooperate to regulate the binding of Ca^{2+}. This interaction may be an isotype-specific intramolecular event. Apparently swapping the V5 domain of PKC-δ and -ε might disrupt such an intramolecular interaction and therefore abolish their isoform-specific functions in 32D cells.

Materials and Methods

Construction of PKC-δ/εV5 and -ε/δV5

The V1-C4 and V5 fragments from PKC-δ and -ε were obtained using PCR with primers directed to the 5′ and 3′ ends of the PKC-δ and -ε fragments. The sequences and locations of the primers are as follows: for the δV1-C4 fragment, 5′δreg (sense) GAA TTC TCC ATC ATG GCA CCC and 3′δC4 (antisense) TGA TAG TCT TGA AAA A; for the εV1-C4 fragment, 5′εreg (sense) GAA TTC ACC ATG GTA GTG TTC AAT and 3′εV5 (antisense) CTG CTC CAG CAG TAC CCA GT; for the δV5 fragment, 5′δV5 (sense) ACT GGT CCC TCC TGG AGA AG and 3′δkin (antisense) GAA TTC CTT AAT TAA ATG TCC; for the εV5 fragment, 5′εV5 (sense) ACT GGG TAC TGC TGG AGC AG and 3′εkin (antisense) GAA TTC TGA AGC AGT TTC TCA. A PCR Optimizer kit (Promega, Madison, WI) was used to find the optimal pH and Mg^{2+} concentrations for each reaction, and *Pfu* DNA polymerase (Stratagene, Menasha, WI) was employed. One hundred nanograms of the cloned mouse PKC-δ and -ε cDNA (3, 36) were used as templates. PCR conditions were as follows: 30 cycles of 1 min at 95°C, 2 min at 58°C, and 3 min at 75°C. The PKC-δ/εV5 and -ε/δV5 chimeras (Fig. 1) were obtained by blunt-end ligation of δ and ε fragments followed by a second round of PCR amplification using the 5′ and 3′ end primers. PCR products were initially cloned into a pBlueScript SK (+/−) vector (Stratagene), sequenced (United States Biochemical Corp., Cleveland, OH), and finally recloned into two expression vectors, pLTR and pMTH, at the *Eco*RI cloning site. pLTR is a mammalian expression vector based on the Harvey sarcoma virus long terminal repeat, which contains the selectable marker xanthine-guanine phosphoribosyltransferase (39). M-δ and H-δ, the 32D lines of PKC-δ overexpressers that use the pMTH (2) and pHM6 (Roche Diagnostics Corp., Indianapolis, IN) vectors to expresses different levels of PKC-δ protein, were used for comparison with the pLTR-based L-δ overexpresser in 32D cells (Fig. 4).

To construct COOH-terminal Myc epitope-tagged proteins, both PKC-δ/εV5 and -ε/δV5 were subcloned into the *Xho*I/*Kpn*I site of a pcDNA3.1/Myc-His(−) B vector (Invitrogen, San Diego, CA) with or without a stop codon incorporated prior to the Myc epitope. To construct COOH-terminal GFP fusion constructs of PKC-δ and -ε and their chimeras, cDNA fragments with *Xho*I on the 5′ end and *Mlu*I on the 3′ end were produced by PCR. After digestion with *Xho*I/*Mlu*I, the chimeric fragments were subcloned into the expression vector pEGFP-N1 (Clontech Laboratories, Inc., Palo Alto, CA) that was modified by inserting a *Mlu*I linker into the plasmid digested with *Sma*I. The correct sequences of the parental and chimeric PKC constructs were verified by sequencing (DNA minicore; Center for Cancer Research, National Cancer Institute, NIH).

Overexpression of Wild-Type PKC and Chimeras in NIH 3T3, 32D, and A7r5 Cells

The 32D cells were grown in RPMI 1640 supplemented with 10% fetal bovine serum (FBS), 5% conditioned medium from WEHI-3 cells as a source of interleukin-3, 4 mM L-glutamine, 100 units/ml penicillin, and 100 μg/ml streptomycin. NIH 3T3 and A7r5 cells were grown in DMEM containing 10% FBS, 4 mM L-glutamine, 100 units/ml penicillin, and 100 μg/ml streptomycin. 32D lines were transfected with PKC constructs by electroporation (400 V, 50 μF). NIH 3T3 cells were transfected by LipofectAMINE Plus (Invitrogen). A7r5 cells were transfected using SuperFect Transfection Reagent (Qiagen, Inc., Valencia, CA). The 32D cells transfected with pLTR-based constructs were selected for 2 weeks in medium supplemented with 0.2 mM hypoxanthine, 0.4 mM aminopterin, and 16 mM thymidine plus 80 μM mycophenolic acid. This yielded the chimera-overexpressing cell line L-δ/εV5. Cells transfected with

pcDNA-based constructs were selected with medium containing 0.5 μg/ml G418. This yielded the chimera-overexpressing cell lines pcDNA, pcDNA-δ/εV5, and pcDNA-ε/δV5. The PKC-δ and -ε overexpressers, 32DL-δ and 32DL-ε, have been described elsewhere (2, 3). The presence of the PKC proteins and the levels of their expression were determined by Western blot analysis.

Western Blot Analysis

Cells (8×10^6) were pelleted and lysed in 400 μl of lysis buffer [10 mM Tris-HCl (pH 7.5), 1 mM EGTA, 1 mM phenylmethylsulfonyl fluoride, and 1% Triton X-100] followed by 10-s sonication. Protein content was monitored by a microprotein assay using the BCA Protein Assay Kit (Pierce Chemical Co., Rockford, IL). Approximately 20 μg of lysates were mixed with equal volumes of 2× SDS sample loading buffer [60 mM Tris-HCl (pH 7.5), 2 mM EDTA, 10 mM 2-mercaptoethanol, 20% glycerol, and 2% SDS], size fractionated by electrophoresis on 4–20% Tris-glycine gels at 100 V for 2 h followed by electrotransfer onto a nitrocellulose membrane at 25 V for 2 h. The membrane was preblotted with a 5% solution of dry milk in Tris-buffered saline [50 mM Tris-HCl and 150 mM NaCl (pH 7.5)] at room temperature for 1 h. The blots were probed with rabbit antisera raised against the COOH terminus of PKC-δ (Research & Diagnostic Antibodies, Berkeley, CA) and against the COOH terminus of PKC-ε (Invitrogen) or with a mouse monoclonal antibody directed against the c-Myc epitope (Santa Cruz Biotechnology, Inc., Santa Cruz, CA). Goat anti-rabbit IgG and goat anti-mouse IgG, coupled to horseradish peroxidase (1:1000; Bio-Rad Laboratories, Hercules, CA), were used as the secondary antibodies. Bands were visualized by the enhanced chemiluminescence Western blotting detection system (Amersham Pharmacia Biotech, Arlington Heights, IL).

Differentiation Assay

32D cells were treated with 10 ng/ml PMA (16.2 nM) for 10–20 h to induce macrophage differentiation. To assess morphology, cytospins of $2-5 \times 10^5$ PMA-treated and untreated cells were stained with Giemsa (Sigma Chemical Co., St. Louis, MO) and images were collected using an upright bright-field microscope under high magnification.

Flow Cytometry Analysis

32D (1×10^6) cells treated with or without 10 ng/ml PMA for 10 h were incubated with anti-Mac-1 (CD11b, M1/70) and anti-Mac-3 (M3/84) antibodies (BD Biosciences, San Diego, CA) conjugated with FITC at 4°C for 30 min. Cells were subsequently analyzed for surface expression of these antigens using a Becton Dickinson FACScan (San Jose, CA). Cells incubated without antibodies or with an irrelevant isotype-matched antibody, FITC anti-mouse CD45R/B220 (BD Biosciences), were used as negative controls.

Apoptosis Assays

Apoptosis in A7r5 cells was initially assayed as described previously (12). Briefly, cells were treated with 2 μm PMA for 4 h, and nuclear DNA condensation was visualized by staining with 0.5 μg/ml Hoechst 33342 for 30 min. For analysis, cells were harvested by scraping off the culture dish, spun down at 400 × *g*, and washed once with PBS. Cell pellets were resuspended in 5% Mowiol 40-88 (Aldrich Chemical Co., Milwaukee, WI) in PBS. A drop of 10 μl was spread on a glass microscope slide, mounted, and examined under a fluorescent microscope. Green cells (≥100) were randomly selected and individually checked for nuclear integrity in each experiment. Cells with intact nuclei were counted as nonapoptotic, and cells with condensed DNA or completely disintegrated nuclei were counted as apoptotic. Cells with these characteristic nuclear changed were enumerated and reported as the percentage of the total GFP-positive cells.

In addition, the TUNEL assay was used to detect apoptotic cells. Forty-eight hours prior to the experiments, A7r5 cells were transiently transfected with GFP-tagged PKC-δ and -ε or their chimeras using LipofectAMINE 2000 (Invitrogen). After two washes in warm growth medium, A7r5 cells were treated with 2 μM PMA for 4 h in a humidified 5% CO_2 incubator. TUNEL analysis was performed using the *in situ* Cell Death Detection Kit tetramethyl rhodamine (Roche Molecular Biochemicals, Indianapolis, IN) according to the manufacturer's protocol. Fluorescent microscopy was performed using a 60× objective, and TUNEL-positive cells containing GFP were identified by colocalization with Hoechst 33342 and by morphology. TUNEL-positive cells were enumerated and reported as the percentage of the total GFP-positive cells.

Confocal Fluorescent Microscopy

Prior to observation, transiently transfected NIH 3T3 cells were washed twice with standard medium (DMEM without phenol red supplemented with 1% FBS) prewarmed to 37°C. All PKC activators were diluted to specified concentrations in the same medium, and the final concentration of solvent (DMSO) was always <0.01%. To image live cells, a Bioptechs Focht Chamber System (FCS2) was inverted and attached to the microscope stage with a custom stage adapter in the confocal minicore (Center for Cancer Research, National Cancer Institute, NIH). NIH 3T3 cells, cultured on a 40-mm round coverslip, were introduced into the chamber system, which was connected to a temperature controller set at 37°C, and medium was perfused through the chamber with a Model P720 microperfusion pump (Instech, Plymouth Meeting, PA). As indicated, the perfusate to the chamber was changed to that containing the specified reagent in the standard medium. Sequential images of the same cell were collected at 1-min intervals using LaserSharp software through a Bio-Rad MRC 1024 confocal scan head mounted on a Nikon Optiphot microscope with a 60× planapochromat lens (Melville, NY). Excitation at 488 nm was provided by a krypton-argon gas laser with a 522/32 emission filter for green fluorescence.

Quantitation of GFP-Tagged PKCs

The confocal images were processed and analyzed using Scion Image (Scion Corp., Frederick, MD). Fixed small, representative areas in the cytoplasm, nucleus, and plasma membrane were selected, and the mean fluorescent intensities were determined. The ratio of nuclear/cytoplasmic distribution

was calculated as the ratio of I_{nucl}/I_{cyto}, where I_{nucl} is the mean fluorescent intensity in the nucleus in a given area and I_{cyto} is the mean fluorescent intensity in a comparable area of the cytoplasm. The extent of membrane translocation was calculated as the ratio of $(I_m - I_{cyto})/I_{cyto}$, where I_m is the mean fluorescent intensity on the plasma membrane in a given area and I_{cyto} is the mean fluorescent intensity in a comparable area of the cytoplasm.

Acknowledgments

We thank Susan Garfield for help with the use of the fluorescent microscope for live cell imaging and Barbara Taylor for assistance in flow cytometry analysis.

References

1. Nishizuka Y. Intracellular signaling by hydrolysis of phospholipids and activation of protein kinase C. Science, 1992;258:607–14.

2. Mischak H, Pierce JH, Goodnight J, Kazanietz MG, Blumberg PM, Mushinski JF. Phorbol ester-induced myeloid differentiation is mediated by protein kinase C-α and δ and not by protein kinase C-βII, ε, ζ, and η. J Biol Chem, 1993;268:20110–5.

3. Mischak H, Goodnight J, Kolch W, et al. Overexpression of protein kinase C-δ and -ε in NIH3T3 cells induces opposite effects on growth, morphology, anchorage dependence, and tumorgenicity. J Biol Chem, 1993;268:6090–6.

4. Cacace AM, Guadagno SN, Krauss RS, Fabbro D, Weinstein IB. The ε isoform of protein kinase C is an oncogene when overexpressed in rat fibroblasts. Oncogene, 1993;8:2095–104.

5. Perletti GP, Folini M, Lin H-C, Mischak H, Piccinini F, Tashjian AH Jr. Overexpression of protein kinase C ε is oncogenic in rat colonic epithelial cells. Oncogene, 1996;12:847–54.

6. Parker PJ, Kour G, Marais RM, et al. Protein kinase C—a family affair. Mol Cell Endocrinol, 1989;65:1–11.

7. Sugden D, Vanecek J, Klein DC, Thomas TP, Anderson WB. Activation of protein kinase C potentiates isoprenaline-induced cyclic AMP accumulation in rat pinealocytes. Nature, 1985;314:359–61.

8. Disatnik MH, Jones SN, Mochly-Rosen D. Stimulus-dependent subcellular localization of activated protein kinase C; a study with acidic fibroblast growth factor and transforming growth factor-β 1 in cardiac myocytes. J Mol Cell Cardiol, 1995;27:2473–81.

9. Goodnight JA, Mischak H, Kolch W, Mushinski JF. Immunocytochemical localization of 8 protein kinase C isozymes overexpressed in NIH3T3 fibroblasts—isoform-specific association with microfilaments, Golgi, endoplasmic-reticulum, and nuclear and cell-membranes. J Biol Chem, 1995;270:9991–10001.

10. Newton AC. Protein kinase C, structure, function and regulation. J Biol Chem, 1995;270:28495–8.

11. Watanabe T, Ono Y, Taniyama Y, et al. Cell division arrest induced by phorbol ester in CHO cells overexpressing protein kinase C-δ subspecies. Proc Natl Acad Sci USA, 1992;89:10159–63.

12. Goerke A, Sakai N, Gutjahr E, et al. Induction of apoptosis by protein kinase Cδ is independent of its kinase activity. J Biol Chem, 2002;277:32054–62.

13. Reyland ME, Anderson SM, Matassa AA, Barzen KA, Quisell DO. Protein kinase Cδ is essential for etoposide-induced apoptosis in salivary gland acinar cells. J Biol Chem, 1999;274:19115–23.

14. Wang QJ, Acs P, Goodnight J, et al. The catalytic domain of protein kinase C-δ in reciprocal δ and ε chimeras mediates phorbol ester-induced macrophage differentiation of mouse promyelocytes. J Biol Chem, 1997;272:76–82.

15. Wang QJ, Acs P, Goodnight J, Blumberg PM, Mischak H, Mushinski JF. The catalytic domain of PKC-ε, in reciprocal PKC-δ and -ε chimeras, is responsible for conferring tumorgenicity to NIH3T3 cells, whereas both regulatory and catalytic domains of PKC-ε contribute to *in vitro* transformation. Oncogene, 1998;16:53–60.

16. DeVries TA, Neville MC, Reyland ME. Nuclear import of PKC δ is required for apoptosis: identification of a novel nuclear import sequence. EMBO J, 2002;21:6050–60.

17. Lorenzo PS, Bogi K, Acs P, Pettit GR, Blumberg PM. The catalytic domain of protein kinase C-δ confers protection from down-regulation induced by bryostatin 1. J Biol Chem, 1997;272:33338–43.

18. Acs P, Wang QJ, Bogi K, et al. Both the catalytic and regulatory domains of protein kinase C chimeras modulate the proliferation properties of NIH3T3 cells. J Biol Chem, 1997;272:28793–9.

19. Hocevar BA, Fields AP. Selective translocation of βII protein kinase C to the nucleus of human promyelocytic (HL60) leukemia cells. J Biol Chem, 1991; 266:28–33.

20. Chalfant CE, Mischak H, Watson JE, et al. Regulation of alternative splicing of protein kinase C-β by insulin. J Biol Chem, 1995;270:13326–32.

21. Blobe GC, Stribling DS, Fabbro D, Stabel S, Hannun YA. Protein kinase C-βII specifically binds to and is activated by F-actin. J Biol Chem, 1996;271: 15823–30.

22. Gökmen-Polar Y, Fields AP. Mapping of a molecular determinant for protein kinase C βII isozyme function. J Biol Chem, 1998;273:20261–6.

23. Svensson K, Zeidman R, Troller U, Schultz A, Larsson C. Protein kinase C β1 is implicated in the regulation of neuroblastoma cell growth and proliferation. Cell Growth & Differ, 2000;11:641–8.

24. Wang QJ, Bhattacharyya D, Garfield S, Nacro K, Marquez VE, Blumberg PM. Differential localization of protein kinase C δ by phorbol esters and related compounds using a fusion protein with green fluorescent protein. J Biol Chem, 1999;274:37233–9.

25. Brodie C, Blumberg PM. Regulation of cell apoptosis by protein kinase C δ. Apoptosis, 2003;8:19–27.

26. Walker SD, Murray NR, Burns DJ, Fields AP. Protein kinase C chimeras—catalytic domains of α-protein kinase C and β(II)-protein kinase C contain determinants for isotype-specific function. Proc Natl Acad Sci USA, 1995; 92:9156–60.

27. Acs P, Bogi K, Lorenzo PS, et al. The catalytic domain of protein kinase C chimeras modulates the affinity and targeting of phorbol ester-induced translocation. J Biol Chem, 1997;272:22148–53.

28. Ono Y, Kurokawa T, Fujii T, et al. Two types of complementary DNAs of rat brain protein kinase C. Heterogeneity determined by alternative splicing. FEBS Lett, 1986;206:347–52.

29. Ono Y, Kikkawa U, Ogita K, et al. Expression and properties of two types of protein kinase C: alternative splicing from a single gene. Science, 1987;236:1116–20.

30. Stebbins EG, Mochly-Rosen D. Binding specificity for RACK1 resides in the V5 region of βII protein kinase C. J Biol Chem, 2001;276:29644–50.

31. Chalfant CE, Ohno Shigeo, Konno Y, et al. A carboxy-terminal deletion mutant of protein kinase C βII inhibits insulin-stimulated 2-deoxyglucose uptake in L6 rat skeletal muscle cells. Mol Endocrinol, 1996;10:1273–81.

32. Martelli AM, Sang N, Borgatti P, Capitani S, Neri LM. Multiple biological responses activated by nuclear protein kinase C. J Cell Biochem, 1999;74:499–521.

33. Blass M, Kronfeld I, Kazimirsky G, Blumberg PM, Brodie C. Tyrosine phosphorylation of protein kinase C δ is essential for its apoptotic effect in response to etoposide. Mol Cell Biol, 2002;22:182–95.

34. Bharti A, Kraeft SK, Gounder M, et al. Inactivation of DNA-dependent protein kinase by protein kinase C δ: implications for apoptosis. Mol Cell Biol, 1998;18:6719–28.

35. Cross T, Griffiths G, Deacon E, et al. PKC-δ is an apoptotic lamin kinase. Oncogene, 2000;19:2331–7.

36. Mischak H, Bodenteich A, Kolch W, Goodnight J, Hofer F, Mushinski JF. Mouse protein kinase C-δ, the major isoform expressed in mouse hematopoietic cells, sequence of the cDNA, expression patterns, and characterization of the protein. Biochemistry, 1991;30:7925–31.

37. Edwards AS, Faux MC, Scott JD, Newton AC. Carboxyl-terminal phosphorylation regulates the function and subcellular localization of protein kinase C βII. J Biol Chem, 1999;274:6461–8.

38. Edwards AS, Newton AC. Phosphorylation at conserved carboxyl-terminal hydrophobic motif regulated the catalytic and regulatory domains of protein kinase C. J Biol Chem, 1997;272:18382–90.

39. Megidish T, Mazurek NA. Mutant protein kinase C that can transform fibroblasts. Nature, 1989;342:807–11.

Molecular Cancer Research

The V5 Domain of Protein Kinase C Plays a Critical Role in Determining the Isoform-Specific Localization, Translocation, and Biological Function of Protein Kinase C-δ and - ε

Qiming Jane Wang, Ganwei Lu, Walter A. Schlapkohl, et al.

Mol Cancer Res 2004;2:129-140.